# Femtosecond laser generation and detection of high-frequency acoustic phonons in GaAs semiconductors

P. Babilotte, P. Ruello,* D. Mounier, T. Pezeril, G. Vaudel, M. Edely, J-M. Breteau, and V. Gusev
*Laboratoire de Physique de l'Etat Condensé, UMR CNRS 6087, Université du Maine, 72085 Le Mans, France*

K. Blary
*Institut d'Electronique, de Microélectronique et de Nanotechnologie (IEMN), UMR CNRS 8520, 59652 Villeneuve d'Ascq Cedex, France*
(Received 25 January 2010; revised manuscript received 14 April 2010; published 15 June 2010)

The experimental detection of short picosecond photoacoustic response induced by femtosecond laser pump radiation deeply penetrating in GaAs and generating long acoustic strain pulse is reported. It is demonstrated that it is possible, in this case, to achieve high-frequency coherent acoustic phonon monitoring in semiconductors as efficiently as in the case of metals where the penetration depth of pump radiation is shorter and the generated acoustic strain pulse is short itself. The physical origin of such monitoring of high-frequency acoustic phonons is discussed thanks to a detailed analysis of the spectral transformation functions of both the generation process (opto-acoustic transformation) and the detection process (acousto-optic transformation). We show that it is possible to tune the detection process from a narrowband to a broadband spectrum detection process. In particular, the broadband detection process is achieved with a proper choice of the probe wavelength permitting efficient coupling between the acoustic field and the probe electromagnetic wave only in a nanometric thin region near semiconductor surface. Efficient broadband acousto-optic detection results in the short pulsed photoacoustic responses in transient optical reflectivity even when long acoustic pulses are generated, because of sufficient sensitivity to high-frequency coherent phonons even weakly contributing to the total acoustic field. These results indicate the opportunity to broaden the range of the substrate materials and pump laser frequencies that can be used in high-frequency coherent phonon spectroscopy of the materials and nanostructures.

DOI: 10.1103/PhysRevB.81.245207 PACS number(s): 78.20.hc, 78.20.hb, 78.20.Pa, 78.47.J−

## I. INTRODUCTION

Picosecond laser ultrasonics is a domain of interdisciplinary research where femtosecond laser pulses are applied for opto-acoustic (OA) generation and acousto-optic (AO) detection of elastic waves in materials.[1–4] The application goal of using femtosecond all-optical pump-probe technique is to monitor the interaction with a tested material or a mechanical structure of the acoustic waves from the GHz-few THz range of frequencies. The word *monitoring* is used in order to indicate that to study the interaction of high frequency waves (of hypersound) with materials it is necessary to develop both the methods of generation and detection of these high-frequency acoustic waves. Multiple experiments conducted after pioneering ones[1,5,6] demonstrated that application of femtosecond laser-based pump-probe technique provides opportunity to reach both goals, i.e., the hypersound can be both generated through the OA effect and detected through the AO effect. In picosecond laser ultrasonics, these are coherent acoustic pulses that are generated, so, in principle, pulsed laser radiation always excites acoustic waves from the GHz-few THz range of frequencies. However these high frequencies contribute to an important part to the total acoustic field of the strain pulse only if the penetration depth of the pump laser radiation is sufficiently short. That is why the common tendency in picosecond laser ultrasonics is to use for the generation of high-frequency phonons the metals or the semiconductors with the energy gap sufficiently lower than the pump laser energy quantum. The situation with acousto-optic detection of coherent phonons is qualitatively similar to their generation in the sense that, in principle, all acoustic frequencies can be detected, but in order to achieve broadband AO transformation at GHz-few THz frequencies range, that is to get an important contribution of hypersound to the total detected signal, it is necessary to use for the detection the materials with shortest penetration depths of the probe laser radiation. It is through the combination of weakly penetrating pump and probe laser pulses that the ultrashort pulsed variations in transient optical reflectivity, which namely corresponds to the generation and detection of high-frequency phonons, are commonly observed. Here below through the experiments in GaAs and the development of the supporting theory we demonstrate that for the monitoring of the high-frequency phonons through the detection of the ultrashort pulsed transients in the optical reflectivity signals, it is not necessary to generate ultrashort strain pulses. If the sensitivity of the wide-band AO detection is high enough in the GHz frequency range then it is still possible to monitor high-frequency phonons contributing (weakly) to long photogenerated strain pulses through the detection of the ultrashort pulsed transient reflectivity signals. From the point of view of application of picosecond laser ultrasonics in phonon spectroscopy of the materials and nanostructures our finding broadens the range of the substrate materials and pump optical frequencies that can be used for monitoring of the high-frequency phonons. In the following parts of the introduction, we provide more quantitative description of the general physical principles of OA generation and AO detection as well as multiple references on the earlier experiments conducted in the ways which are

 ©2010 The American Physical Society

currently usual for picosecond laser ultrasonics. In this analysis, we use the formalism of the spectral transformation function of OA conversion[4,7] and we introduce the formalism of spectral transformation function of AO conversion.[8]

### A. Opto-acoustic conversion

The spectral transformation function of opto-acoustic conversion $K_{\mathrm{OA}}(\omega)$ (Refs. 4 and 7) determines how efficiently the different cyclic frequencies $\omega$ contained in the spectrum $\tilde{f}(\omega)$ of the laser pulse intensity envelope $f(t/\tau_L)$ ($\tilde{f}(\omega)=\int_{-\infty}^{+\infty} f(t/\tau_L)\exp(i\omega t)dt$, where $\tau_L$ is the characteristic duration of the laser pulse) are transformed into acoustic frequencies in the OA conversion process. When femtosecond laser pulses are applied for generation of acoustic waves their direct interaction with the material can be considered as instantaneous at the time scale corresponding to GHz frequency range. Then $f(t/\tau_L)$ can be approximated by the delta function $f(t/\tau_L)\approx\tau_L\delta(t)$, correspondingly $\tilde{f}(\omega)\approx$const, and the spectrum $\tilde{\eta}(\omega)$ of the photogenerated acoustic strain pulse replicates the spectrum transformation function of OA conversion $\tilde{\eta}(\omega)=K_{\mathrm{OA}}(\omega)\tilde{f}(\omega)\sim K_{\mathrm{OA}}(\omega)$. It is well established[1,4,7] that in order to convert into acoustic frequencies the highest frequencies from the available excitation spectrum $\tilde{f}(\omega)$ it is necessary to use pump optical radiation weakly penetrating in the material, i.e., with the highest possible values of the imaginary part $k_g''$ of the optical wave number $k_g=k_g'+ik_g''$. Here and in the following, $k$ is the wave number of optical or acoustical waves, while $k'$ and $k''$ denote its real and imaginary parts, respectively. The index "$g$" attributes the wave number to generation process, i.e., to optical wave used for the generation of acoustic waves, and will attribute in the following the acoustic frequencies $\omega$ to generated ones. In addition to the use of materials with the shortest possible pump light intensity penetration depth $\alpha_g^{-1}=(2k_g'')^{-1}$ it is necessary to avoid materials where the transport of absorbed laser energy outside the pump light penetration depth $\alpha_g^{-1}$ can take place at supersonic velocities. For example, fast supersonic transport of energy can be due to diffusion of overheated nonequilibrium electrons in bold metals[9–12] or photogenerated electron-hole plasma in semiconductors.[13,14] If the supersonic transport of energy is avoided then the spectrum of the efficiently photogenerated hypersound can extend up to the frequencies at which the acoustic wave number $k_a(\omega)=\omega/v_a$ is equal to the laser pump intensity absorption coefficient $k_a(\omega)=\alpha_g=2k_g''$, i.e., up to the frequencies $\omega_g=\alpha_g v_a=2k_g'' v_a$. Here and in the following the index "$a$" attributes the wave number to acoustical waves, where $v_a$ is the velocity of the acoustic wave. Correspondingly the characteristic duration of the photogenerated acoustic pulses can be as short as the time $\tau_g$ of acoustic wave propagation across the pump laser intensity penetration depth $\tau_g=\omega_g^{-1}=(2k_g'' v_a)^{-1}$. From mathematics point of view, all these relations are due to the existence of the factors $(\omega\pm i\omega_g)^{-1}$ in the spectral transformation function of OA conversion $K_{\mathrm{OA}}(\omega)$, i.e., $K_{\mathrm{OA}}(\omega)$ contains the contributions proportional to $(\omega+i\omega_g)^{-1}$ and/or $(\omega-i\omega_g)^{-1}$ and the imaginary characteristic frequencies $\pm i\omega_g$ determine some of the poles of the spectral transformation function on the complex $\omega$ plane.

### B. Acousto-optic conversion

The spectral transformation function of acousto-optic conversion $K_{\mathrm{AO}}(\omega)$ determines how efficiently different acoustic frequencies, contained in the acoustic field entering the detection volume, can be converted in the spectrum of, for example, intensity variation of the reflected probe laser radiation penetrating in this volume. The femtosecond probe laser pulses delayed in time relative to pump laser pulses provide, through the variation of the delay time, an opportunity to detect acoustically induced variations in optical reflectivity with a time resolution equal to the duration of the probe laser pulse $\tau_L$. However, the spectral transformation function of AO conversion $K_{\mathrm{AO}}(\omega)$ depends not on the distribution in depth of the probe laser intensity, as it is in the case of $K_{\mathrm{OA}}(\omega)$, but on the spatial distribution of laser electric field. This difference takes place because in contrast to OA effect, which depends on optical intensity both in the case of thermoelastic and deformation potential mechanisms of OA conversions,[4,7] AO effect depends on the laser electric field. As a consequence the characteristic acoustic frequency $\omega_d$ of AO conversion is determined by the equality of the acoustic wave number $k_a(\omega)=\omega/v_a$ and $2(k_d''-ik_d')$ of the probe laser radiation, i.e., not by $k_a(\omega)=\omega/v_a=2k_d''$ as it could be proposed by erroneously assuming complete analogy with the generation process, because the real part $k_d'$ of the complex wave number $k_d=k_d'+ik_d''$ also plays role. The index "$d$" attributes here and in the following the wave number to detection process, i.e., to optical wave used for the detection of acoustic waves, and attributes the acoustic frequencies $\omega$ to generated ones. As a result the characteristic acoustic frequency $\omega_d$ of AO conversion is complex because the optical wave number is complex: $\omega_d=\omega_d''-i\omega_d'=-i2k_d v_a=2k_d'' v_a-i2k_d' v_a$. As it can be seen from the presentation of the AO detection process in the frequency domain,[8] the spectral transformation function of AO conversion $K_{\mathrm{AO}}(\omega)$ contains a factor $(\omega+i\omega_d)^{-1}=(\omega+\omega_d'+i\omega_d'')^{-1}=(\omega+2k_d' v_a+i2k_d'' v_a)^{-1}$ with a pole at the characteristic complex frequency $-i\omega_d$. Here $\omega_d'$ and $\omega_d''$ are the characteristic acoustic frequencies related to the real and imaginary parts of the probe optical wave number, respectively. This circumstance leads to the following important consequences. The first one is that in order to broaden the frequency bandwidth of the AO detection, i.e., to broaden $K_{\mathrm{AO}}(\omega)$, it is necessary to use probe laser radiation with the largest possible wave numbers. In practice this is achieved through increasing the imaginary part $k_d''$, by making for a particular material a choice of highly absorbed probe optical quanta[15] or by choosing a highly opaque materials for a particular probe laser quanta.[1,11,12,16,17] The second consequence is that the pole $\omega=-i\omega_d$ of the $K_{\mathrm{AO}}(\omega)$ in the frequency domain results in the presence, in the acoustic signal monitored in the time domain, of the transients with two different characteristic time scales, first one equal to the time of sound propagation across the laser probe intensity penetration depth $\tau_d''=(\omega_d'')^{-1}=(2k_d'' v_a)^{-1}$ and the second one proportional to the

time of sound propagation across the laser probe wavelength in the material $\tau'_d=(\omega'_d)^{-1}=(2k'_d v_a)^{-1}$.

### C. State-of-art in picosecond laser ultrasonics

Picosecond laser ultrasonics experiments reported until now (see, for example, the recent publications[16–20] and the references therein) confirm the discussed above qualitative theoretical model. Because for the monitoring of hypersonic waves they should be first generated, then substrates or films highly absorbing pump laser radiation are commonly used for OA launching of the hypersound inside a material or inside a mechanical structure. However, in the part of AO detection, two different configurations are typical to already reported experiments.

In the first configuration the detection takes place in a material, which highly attenuates probe optical radiation, and AO conversion can be considered as being strongly localized in the vicinity of the surface if the imaginary part of the optical probe wave number $k''_d$ is much larger than the wave numbers $k_a(\omega)=\omega/v_a$ in the acoustic field arriving in the detection region after the propagation inside the material. This situation is typical, for example, to most of the experiments where both the generation and the detection of hypersound is achieved at the same optical wavelength and in the same material,[1,8,9,11,15] because the generated acoustic pulse is usually much broader in space than the optical pump penetration depth $(2k''_g)^{-1}$ due to supersonic redistribution of absorbed laser energy in metals[8,9,11,18,19] and semiconductors,[13,14,20] and it can be also additionally broadened in propagation due to preferential absorption of high frequencies.[18,19] Then it appears that $k_a(\omega)=\omega/v_a \ll 2k''_g=2k''_d$. In this configuration, where the optical probe attenuation coefficient $2k''_d$ significantly exceeds the wave numbers $k_a(\omega)$ in the acoustic field, the detected temporal changes in intensity of optical reflection replicate the time profile of the acoustic strain pulse, if the AO detection is at the interface of opaque and transparent materials,[17,19,21] and its time derivative if the detection is at a mechanically free surface of an opaque material.[1,2,8–11] The spectral transformation function of AO conversion $K_{\mathrm{AO}}(\omega)$ is $K_{\mathrm{AO}}(\omega)\sim\omega^0$ and $K_{\mathrm{AO}}(\omega)\sim\omega$ for the detection at the mechanically loaded and mechanically free surfaces, respectively. In both cases the detection provides access to high frequencies in the spectrum of the incident acoustic pulse and, consequently, the AO detection does not limit the spectrum of the monitored hypersound. Thus the spectrum of the monitored acoustic waves in this first typical configuration of picosecond laser ultrasonics experiments is controlled by the processes of hypersound generation and propagation.

In the second typical picosecond laser ultrasonics configuration, the detection is achieved by deeply penetrating probe radiation, i.e., $k''_d \ll k'_d$, with $k''_d$ being much smaller than the characteristic wave numbers $k_a(\omega)=\omega/v_a$ in the acoustic field to be detected, i.e., after the acoustic field generation and propagation. This configuration is commonly realized in the experiments with transparent films on opaque substrates[22–26] or opaque films on transparent substrates[2,3,15,25,27] when the generation of hypersound takes place in the opaque material while its detection takes place in the transparent material. In this configuration of so-called picosecond acoustic interferometry[2,6] acoustically induced changes in optical reflectivity take place during all the duration $\tau''_d=(\omega''_d)^{-1}=(2k''_d v_a)^{-1}$ of the photogenerated acoustic pulse propagation across the large penetration depth of the probe laser radiation in the case of the transparent thick (semi-infinite) substrate or during complete lifetime of the photogenerated hypersound inside the thin transparent film. The duration of the transient reflectivity signal can be also limited by the coherence time of the probe laser pulses.[2,6] The detected signal has a form of the decaying harmonic (sinusoidal) oscillation with a period $2\pi(\omega'_d)^{-1}$ controlled by the time $\tau'_d=(\omega'_d)^{-1}$ of sound propagation across the optical probe wavelength. In the spectral domain, the detected signal is dominated by this quasimonochromatic oscillation, which takes place at the so-called Brillouin frequency $\omega_B=\omega'_d=2k'_d v_a$. In this case, the spectrum transformation function of AO conversion $K_{\mathrm{AO}}(\omega)$ has an extremely important influence on the spectrum of monitored hypersound through its preferential sensitivity to spectral components of acoustic field in the vicinity of $\omega=\omega_B=\omega'_d$. In the limit $\omega''_d\to 0$ the function $K_{\mathrm{AO}}(\omega)$ has only a nearly real pole $K_{\mathrm{AO}}(\omega)\propto(\omega+\omega'_d)^{-1}$. Although the higher frequencies $\omega>\omega_B=\omega'_d$ of the acoustic field are formally detectable, in practice it is very difficult to monitor them, by filtering the Brillouin frequency out from the detected signal, when their spectral intensities are much lower than the intensity of the Brillouin line. So in this second picosecond laser ultrasonics configuration, where the detection of short acoustic pulses is achieved in optically transparent materials, the spectrum of the monitored hypersound is cut both from above and from below by the detection process and is very narrow. Thus the spectrum and the time profile of the monitored hypersound are controlled by the detection process. The role of the generation process is just to produce the acoustic waves containing spectral components in the vicinity of the Brillouin frequency with sufficient amplitudes for their AO detection. The transition from the second detection configuration to the first one has been demonstrated experimentally by increasing probe light absorption coefficient through tuning the probe laser quantum energy near the onset of interband transition of the semiconducting Si.[15] With diminishing probe light penetration depth, and without any modification of the generation process of short acoustic pulses in a few nanometers thick metallic film, the monitored signal transforms in the time domain from a slowly decaying sinusoidal oscillation into a bipolar short pulse.

### D. Detection of high-frequency coherent acoustic phonons in the case of generation of long acoustic pulses

By the present communication we attract the attention to an earlier unexplored opportunity to monitor propagation of high frequency hypersound through the detection of ultrashort pulsed transient reflectivity signals, even in the case where photogenerated acoustic pulses are relatively long. This situation, realized in some of our picosecond laser ultrasonics experiment in GaAs, can be understood due to the-

oretical development presented in section II. On the one hand, it is similar to situation that takes place in near surface AO detection (i.e., in the first of above discussed configurations), because it can be realized when the characteristic wave numbers in the acoustic field to be detected are much smaller than the absorption coefficient of the probe optical radiation $k_a(\omega)=\omega/v_a \ll 2k_d''$. But on the other hand it is similar to picosecond ultrasonic interferometry (i.e., to the second of above discussed configurations), because the monitored spectrum of hypersound is controlled by the AO detection and the time profiles of the monitored acoustic pulses are governed by the times of sound propagation across the probe light penetration depth $\tau_d''=(\omega_d'')^{-1}=(2k_d''v_a)^{-1}$ and by the Brillouin period $T_B=2\pi\tau_d'=2\pi(\omega_B)^{-1}=2\pi(\omega_d')^{-1}=2\pi(2k_d'v_a)^{-1}$. Theoretical analysis predicts that in the case $k_d''\propto k_d' \gg k_g''$, i.e., when the penetration depth of the probe radiation is much shorter than the penetration depth of the pump radiation, the OA detection is preferentially sensitive to the spectrum of acoustic field, not in the vicinity of a single frequency $\omega=\omega_B$, as it is in picosecond ultrasonic interferometry, but to a relatively large band of frequencies, which is controlled by $\omega_d''$ and $\omega_d'$ through the complex pole $\omega=-i\omega_d=-\omega_d'-i\omega_d''=-2k_d'v_a-i2k_d''v_a$ in the spectral transformation function of AO conversion. As OA generation produces the pulses, which, although being long, contain some, although relatively small, amount of sufficiently high-frequency spectral components, then preferential selection of these high frequencies by the AO detection process provides opportunity to monitor them. In the time domain this monitoring corresponds to the detection of ultrashort pulsed transient reflectivity signals.

The article is organized as follows. In Sec. II, we revisit the theory of AO detection and introduce for the first time the spectral transformation function of AO conversion for the case of AO detection at the interface between the transparent film and opaque substrate. We also provide theoretical predictions for the picosecond ultrasonics signals and discuss the conditions necessary for monitoring of high-frequency coherent acoustic phonons through the detection of ultrashort pulsed transients in optical reflectivity in the case where the photogenerated acoustic pulses are long. In Sec. III, we present the experimental configuration, the samples, and we discuss the optical and acousto-optical properties of GaAs substrate and ZnO film which are essential for the understanding of the processes of OA generation and AO detection in our samples. In Sec. IV, we present the experimental observations. The monitoring of the short pulsed picosecond transients in probe laser reflectivity in the case where the photogenerated acoustic pulses are long is experimentally demonstrated. Section V is devoted to the analysis and discussion. We finally conclude by mentioning some perspectives of this research.

## II. THEORY

The theory of acousto-optic detection developed first for the case of acoustic strain detection at mechanically free surface of a semi-infinite material[1] has been later extended to the case of AO detection in the structure composed of a film on a substrate[8,28] and to the case of multilayered structures.[20,29] The solution for the electromagnetic field complex reflection coefficient variation $\Delta r=r-r_0$, $|\Delta r| \ll |r-r_0|$ (here $r_0$ is the complex reflection coefficient in the absence of the pump laser pulses) has the form:[8]

$$\begin{aligned}\Delta r/r_0 = {} & 2ik_{d0}u(0) + C\left[\left(k_{d1}+\frac{\partial k_{d1}}{\partial \eta}\right)\int_0^H \eta(z,t)dz\right. \\ & + \frac{1}{2}\frac{\partial k_{d1}}{\partial \eta}\int_0^H \eta(z,t)\left[r_{12}e^{2ik_{d1}(H-z)}+\frac{1}{r_{12}}e^{-2ik_{d1}(H-z)}\right]dz \\ & \left. + \frac{1}{2}\frac{\partial k_{d2}}{\partial \eta}\left(\frac{1}{r_{12}}-r_{12}\right)\int_H^\infty \eta(z,t)e^{2ik_{d2}(z-H)}dz\right] \\ = {} & \Delta A/A + i\Delta\phi, \end{aligned} \tag{1}$$

where

$$C = 2i\frac{r_{12}(1-r_{01}^2)}{(r_{01}e^{-ik_{d1}H}+r_{12}e^{ik_{d1}H})(e^{-ik_{d1}H}+r_{01}r_{12}e^{ik_{d1}H})}. \tag{2}$$

Here, and in the following the indexes 0, 1, and 2 are used to attribute the considered physical quantities to air, film or substrate, respectively. Note, that in order to facilitate the reading of the following parts of the article we provide in the Appendix the list of the notations, which are most frequently used in the text. $k_{di}(i=0,1,2)$ are then the wave vectors of the probe light in the air $(i=0)$, in the film $(i=1)$ and in the substrate $(i=2)$. The coefficients $r_{ij}$ $(i,j=0,1,2)$ are the corresponding reflection coefficients of probe light at the interfaces, $u$ is the mechanical displacement in the material [$u(0)$ is the mechanical displacement of the front surface of the film]; $\eta=\partial u/\partial z$ is the longitudinal strain, and $H$ is the thickness of the film in the absence of the photogenerated acoustic field. Equation (1) indicates that both the amplitude $A$ and the phase $\phi$ of the reflection coefficient ($r_0=Ae^{i\phi}$) are influenced by the acoustic field: $\Delta A/A=\mathrm{Re}(\Delta r/r_0)$, $\Delta\phi=\mathrm{Im}(\Delta r/r_0)$. With the definition of optical reflectivity, $R=rr^*$, where "*" denotes the operation of complex conjugation, the formula for the relative variations in light intensity reflectivity is $\Delta R/R=2\ \mathrm{Re}(\Delta r/r_0)$. Here, we analyze a particular experimental configuration where the transparent film is deposited on the opaque substrate (Fig. 1). In accordance with Eq. (1) the contributions to the electric field reflectivity variations $\Delta r/r_0$ are in general provided both by the acoustic fields in the film and in the substrate. The contributions, which are proportional to $k_{di}$ $(i=0,1)$, are interferometric in the sense that they are sensitive to the mechanical displacements of the transparent film boundaries $u(0)=u(z=0)$ and $u(H)=u(z=H)$. The first of these displacements modifies the propagation length of the probe light in air [see the first term in Eq. (1)], while both of them contribute to the modification of the transparent film thickness $\int_0^H \eta dz=u(H)-u(0)=\Delta H$. The contributions to $\Delta r/r_0$, which are proportional to $\partial k_{di}/\partial\eta$ $(i=1,2)$ are acousto-optic. They are controlled by the distribution of strain $\eta(z,t)$ in the acoustic field, the magnitude of acousto-optic (elasto-optic) coefficients $\partial k_{di}/\partial\eta$ and also by the interference effects of the probe optical field inside the transparent film through the complex coefficients

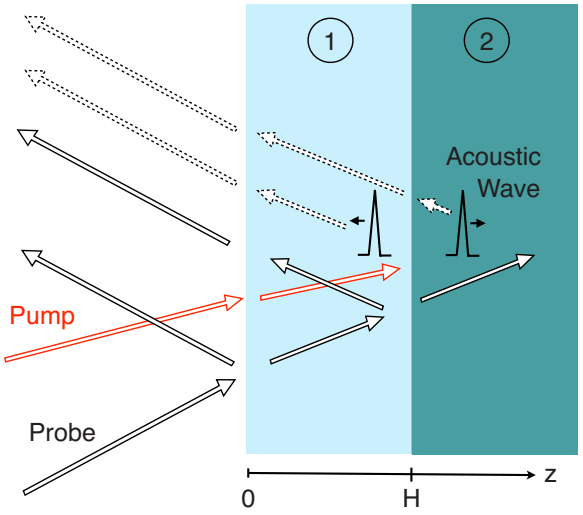


FIG. 1. (Color online) Experimental system: a transparent thin film of thickness H (medium 1), used as a local delay line for acoustic phonon time of flight experiments, is deposited onto an opaque substrate (GaAs, medium 2). The pump beam energy is opto-acoustically converted within the opaque substrate (medium 2). The transient reflectivity of the sample is then monitored with a probe beam delayed in time relatively to the pump beam. The transient reflectivity signal is composed of several contributions. A so-called contribution of interferometric nature is due to free surface and interface displacements caused by propagating acoustic wave [the terms proportional to $k_{d0}$ and $k_{d1}$ in Eq. (1)]. Two photoelastic contributions are due to the coupling between probe light and the acoustic wave within the transparent delay line and within the opaque substrate [last two terms in Eq. (1)] through acousto-optic effect.

in front of $\partial k_{di}/\partial\eta$, in particular through the coefficient $C$ [Eq. (2)]. These coefficients depend on optical properties of the structure and thickness of the film. As the goal of the research presented here is the evaluation of the opto-acousto-optic monitoring of coherent high-frequency phonons in opaque materials, we assume in the theory that acousto-optic effect in transparent film, which can provide strong contribution to the signal at Brillouin frequency of the film material, is negligible $\partial k_{d1}/\partial\eta=0$. In experiment we satisfy this condition by a particular choice of the transparent material (ZnO).[18,21] The theoretical prediction in Eq. (1) simplifies to the following equation where the origin of the coordinate system was shifted to the film/substrate interface:

$$\Delta r/r_0 \approx 2ik_{d0}u(0) + C\left[k_{d1}\Delta H(t) + \frac{1}{2}\frac{\partial k_{d2}}{\partial\eta}\left(\frac{1}{r_{12}} - r_{12}\right)\int_0^\infty \eta(z,t)e^{2ik_{d2}z}dz\right]. \quad (3)$$

The theoretical prediction in Eq. (3) demonstrates that acousto-optic contribution to the electromagnetic field reflectivity variations:

$$\Delta r/r_0 \simeq B\frac{\partial k_{d2}}{\partial\eta}\int_0^\infty \eta(z,t)e^{2ik_{d2}z}dz, \quad (4)$$

where $B=\frac{C(1-r_{12}^2)}{2r_{12}}$, depends not only on the convolution integral $\int_0^\infty \eta(z,t)e^{2ik_{d2}z}dz$ of the acoustic strain distribution $\eta(z,t)$ in the substrate with the so-called sensitivity function $e^{(2ik_{d2}z)}$ of the AO detection near the surface of a semi-infinite media,[1] but it also strongly depends on the photoelastic coefficients of the substrate and on the optical interference phenomena in the transparent film through the coefficient B defined in Eqs. (4) and (2). By presenting the propagating acoustic strain pulse, transmitted from the transparent film into the opaque substrate, in the spectral form $\eta(t,z)=\eta(t-z/v_{a2})=\frac{1}{2\pi}\int_{-\infty}^{+\infty}\tilde{\eta}(\omega)e^{-i\omega(t-z/v_{a2})}d\omega=\frac{1}{2\pi}\int_{-\infty}^{+\infty}\tilde{\eta}(\omega)e^{-i(\omega t-k_{a2}z)}d\omega$, where $v_{a2}$ and $k_{a2}$ are the longitudinal acoustic velocity in the substrate and the acoustic wave number in the substrate, respectively, the convolution integral can be done analytically. The presentation of the electric field reflectivity changes detected through AO effect

$$[\Delta r(t)/r_0]_{\mathrm{AO}} = \frac{1}{2\pi}\int_{-\infty}^{+\infty}[\Delta\tilde{r}(\omega)/r_0]_{\mathrm{AO}}e^{-i\omega t}d\omega \quad (5)$$

in the frequency domain is deduced:

$$[\Delta\tilde{r}(\omega)/r_0]_{\mathrm{AO}} = B\frac{\partial k_{d2}}{\partial\eta}\frac{i}{[k_{a2}(\omega)+2k_{d2}]}\tilde{\eta}(\omega) = \frac{B(\partial k_{d2}/\partial\eta)(iv_{a2})}{[\omega+2k'_{d2}v_{a2}+i2k''_{d2}v_{a2}]}\tilde{\eta}(\omega) = K^r_{\mathrm{AO}}(\omega)\tilde{\eta}(\omega), \quad (6)$$

where $K^r_{\mathrm{AO}}$ denotes the spectral transformation function of AO conversion of acoustic strain into the electromagnetic field complex reflectivity variations.

The presentation in Eq. (6) confirms the statements formulated in Section I, i.e., that the complex pole at $\omega=-2k'_{d2}v_{a2}-i2k''_{d2}v_{a2}=-i\omega_{d2}$ governs AO conversion in the frequency domain.[8] The presentation in Eq. (6) also confirms that $K^r_{\mathrm{AO}}(\omega)$ cuts the AO detected signal at frequencies above $\max(\omega'_{d2},\omega''_{d2})$ because $|K^r_{\mathrm{AO}}(\omega)|\propto[(\omega+\omega'_{d2})^2+(\omega''_{d2})^2]^{-1/2}$. It is worth to be noted that in the frequency domain, the magnitude of the AO transfer function $|K^r_{\mathrm{AO}}(\omega)|$ has a narrow spectrum in the case of probing in transparent medium $k'_{d2}\gg k''_{d2}$ while it becomes broad in an opaque probed medium where $k'_{d2}\sim k''_{d2}$ (Fig. 2). We remind here that $\Phi'$ and $\Phi''$ are used for the real and imaginary parts of the complex function $\Phi$ and the index "$d$" attributes the considered quantity $\Phi_d$ to the detection process.

A complete analysis can be also conducted in the time domain. For the time $t>0$, which corresponds to the time after the first arrival to the substrate of acoustic pulses generated in the substrate, transmitted to the film and reflected at mechanically free surface, the integration in Eq. (5) can be done by closing the integration loop with a half-circle of an infinite radius in the negative part of the complex $\omega$-plane and applying the Cauchy theorem. Then it follows that reflectivity variations in the time domain always contain the contribution

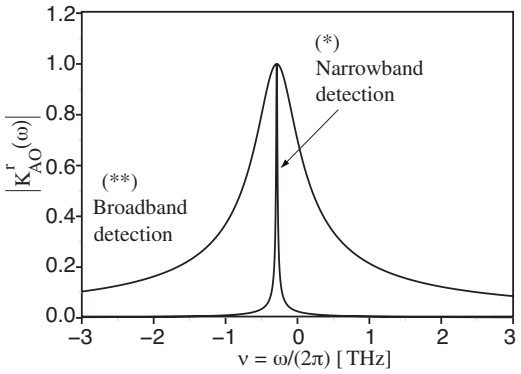


FIG. 2. Normalized amplitude of the spectrum of the AO transfer function for a detection taking place within a transparent ( $^{*}$) and opaque medium ( $^{**}$). The ratio $k'_{d2}/k''_{d2}$ is 40 ( $^{*}$) and 1 ( $^{**}$). $v_{a2}$ is 4830 $ms^{-1}$ and $k'_{d2}=3.10^{7}$ $m^{-1}$

$$[\Delta r(t)/r_0]_{\mathrm{AO}}^{\omega_d} = B\frac{\partial k_{d2}}{\partial \eta} v_{a2}\tilde{\eta}(\omega = -2k'_{d2}v_{a2} - i2k''_{d2}v_{a2}) \times e^{i2k'_{d2}v_{a2}t - 2k''_{d2}v_{a2}t} H_e(t) \tag{7}$$

from the residue in the pole $\omega=-2k'_{d2}v_{a2}-i2k''_{d2}v_{a2}=-i\omega_{d2}$.[30] In Eq. (7), $H_e(t)$ denotes the step function ($H_e(t)=[1+sign(t)]/2$). The solution in Eq. (7) confirms the statements formulated in Sec. I, that there is always a transient AO contribution to the time-domain complex reflectivity that is governed by the Brillouin period $T_{B2}=2\pi\tau'_{d2}=2\pi(\omega_{B2})^{-1}=2\pi(\omega'_{d2})^{-1}=2\pi(2k'_{d2}v_{a2})^{-1}$ and by the time of ultrasound propagation across the probe light penetration depth $\tau''_{d2}=(\omega''_{d2})^{-1}=(2k''_{d2}v_{a2})^{-1}$ independently of how long are the photogenerated acoustic pulses. The duration of the transient reflectivity pulse described by Eq. (7) does not exceed $\tau''_{d2}=(\omega''_{d2})^{-1}=(2k''_{d2}v_{a2})^{-1}$, i.e., the time of acoustic wave propagation across the probe light penetration depth into the substrate. Consequently this contribution to monitored opto-acousto-optic signal can be observed at picoseconds time scale if the laser probe absorption coefficient is sufficiently high.

A very instructive example, which in fact perfectly corresponds to our experiments, is the case where the photogeneration of the acoustic pulse takes place only in the opaque substrate, while the laser-induced generation of acoustic waves in the transparent film, which can be caused by the transport of the absorbed optical energy across the substrate/film interface, is negligible, and also the energy transport in the substrate is subsonic at the scale of pump light penetration depth. It is well known that in this case a strain pulse of exponential time profile with a duration equal to time of sound propagation across the optical pump penetration depth $\tau''_{g2}=(\omega''_{g2})^{-1}=(2k''_{g2}v_{a2})^{-1}$ is launched into the film.[1,4,7,18] The time profile and the frequency spectrum of the strain pulse, which returns in the substrate after the reflection at mechanically free surface have the time profile:

$$\eta(t - z/v_{a_2}) = \eta_0 e^{-(t-z/v_{a_2})/\tau''_{g2}} H_e(t - z/v_{a_2}) \tag{8}$$

and the frequency spectrum

$$\eta(\omega) = \eta_0 \frac{i}{\omega + i(1/\tau_{g''_2})} = \eta_0 \frac{i}{\omega + i\omega_{g''_2}}, \tag{9}$$

respectively.

Here $\eta_0$ is the value of the characteristic strain in the acoustic pulse. By substituting Eq. (9) into Eq. (6), we find the spectrum of complex reflectivity $[\frac{\Delta\tilde{r}(\omega)}{r_0}]_{\mathrm{AO}} = -\eta_0 B\frac{\partial k_{d2}}{\partial \eta} v_{a2}\frac{1}{(\omega+i\omega_{d2})}\frac{1}{(\omega+i\omega''_{g2})}$, which provides opportunity to do the integral in Eq. (5) in the complex plane analytically by the method of residues. The solution for the transient complex AO reflectivity in the time-domain takes the form:

$$\left[\frac{\Delta r(t)}{r_0}\right]_{\mathrm{AO}} = -\eta_0 B\frac{\partial k_{d2}}{\partial \eta} v_{a2}\frac{1}{(\omega_{d2} - \omega''_{g2})} \times [e^{-t/\tau''_{g2}} - e^{i\omega'_{d2}t - t/\tau''_{d2}}] H_e(t). \tag{10}$$

As it could have been expected from the fact that the spectral transformation function of AO conversion cuts high-frequency part of the spectrum, the transient reflectivity in Eq. (10) does not reproduce infinitely short rise time of the strain pulse described in Eq. (8) by the step function $H_e(t-z/v_{a2})$. In fact both the real part $\mathrm{Re}[F(t)]=[e^{-t/\tau''_{g2}}-\cos(\omega'_{d2}t)e^{-t/\tau''_{d2}}]H_e(t)$ and the imaginary part $\mathrm{Im}[F(t)]=[-\sin(\omega'_{d2}t)e^{-t/\tau''_{d2}}]H_e(t)$ of the complex temporal profile, described by the function $F(t)=[e^{-t/\tau''_{g2}}-e^{i\omega'_{d2}t-t/\tau''_{d2}}]H_e(t)$ in Eq. (10), have smooth leading fronts. The analysis of the compact solution in Eq. (10) confirms the statement formulated in Sec. I that, if the attenuation coefficient of the probe radiation is much smaller than that of the pump radiation, resulting in $\tau''_{d2} \gg \tau''_{g2}$ in Eq. (10), then the signal for $t \geq \tau''_{g2}$ is dominated by the Brillouin oscillation, which contributes both to real and imaginary parts of the complex profile $F(t) \simeq -e^{i\omega'_{d2}t-t/\tau''_{d2}}H_e(t)$. The analysis of the solution in Eq. (10) confirms also another statement formulated in Sec. I that in order to resolve acousto-optically the profile of the strain pulse, it is necessary to use the probe radiation which is absorbed in the substrate much stronger than the pump radiation. In this limiting case where the attenuation coefficient of the probe radiation is much larger than that of the pump radiation, resulting in $\tau''_{d2} \ll \tau''_{g2}$ in Eq. (10), i.e., in much shorter time of acoustic wave propagation across the penetration depth of the probe light than across the penetration depth of the pump light, it is the real part of the complex profile $F(t)$ in Eq. (10) which for $t \geq \tau''_{d2}$ reproduces exponential strain pulse profile from Eqs. (8): $\mathrm{Re}[F(t)]=e^{-t/\tau''_{g2}}H_e(t)$. Thus the theory predicts that, in order to resolve acousto-optically the profile of the strain pulse, the optical scheme [i.e., one analyzing the complex reflectivity changes $\Delta r(t)$] in combination with factor coming from the complex coefficient in front of $F(t)$ in Eq. (10) should provide necessary sensitivity to $\mathrm{Re}[F(t)]$.

The theoretical prediction, to which we want to attract attention in this article, is that the imaginary part $\mathrm{Im}[F(t)]=[-\sin(\omega'_{d2}t)e^{-t/\tau''_{d2}}]H_e(t)$ of the temporal profile $F(t)$ in Eq. (10) does not depend at all on the time evolution of the strain field. It means that, if the optical scheme (i.e., one analyzing

the complex reflectivity changes $\Delta r(t)$) together with factor coming from the complex coefficient in front of $F(t)$ in Eq. (10) provides preferential sensitivity to Im$[F(t)]$, then acoustic transients controlled by $T_{B2}$ and $\tau''_{d2}$ can be detected independently of the duration of the photogenerated acoustic pulses, i.e., independently on whether the photogenerated pulses are long or short. These acoustic transients have the form of decaying sinusoidal oscillations if the time of sound propagation across the probe light penetration depth significantly exceeds the Brillouin period in the substrate $\tau''_{d2} \geqslant T_{B2}$ and they have the form of the pulses in the case $\tau''_{d2} \leq T_{B2}$. In the latter case the monitored pulsed transient reflectivity signals can be shorter than the photogenerated acoustic pulses.

In the particular case of our experiments, the optical scheme detects the variations in the amplitude of the complex reflectivity, i.e., it detects the variations in laser intensity reflectivity $\Delta R/R = 2\ \mathrm{Re}(\Delta r/r_0)$. Note that in the general case the spectral function of AO strain transformation into laser intensity variations $K^R_{\mathrm{AO}}(\omega)$, i.e., the factor in the relationship $[\Delta\tilde{R}(\omega)/R]_{\mathrm{AO}} = K^R_{\mathrm{AO}}(\omega)\tilde{\eta}(\omega)$, can be defined with the help of Eq. (5) and accounting for the fact that strain field in the time domain is real, as $K^R_{\mathrm{AO}}(\omega) = (K^r_{\mathrm{AO}}(\omega) + [K^r_{\mathrm{AO}}(-\omega)]^*)$. For the intensity reflectivity in the time domain, using the solution in Eq. (10), we derived:

$$\left[\frac{\Delta R(t)}{R}\right]_{\mathrm{AO}} = \eta_0 \left\{ (\mathrm{Re}\left[\frac{C(\partial k_{d2}/\partial\eta)}{(k_{d2} - k''_{g2})}\right] \times [e^{-t/\tau''_{g2}} - \cos(\omega'_{d2}t)e^{-t/\tau''_{d2}}] + \mathrm{Im}\left[\frac{C(\partial k_{d2}/\partial\eta)}{(k_{d2} - k''_{g2})}\right] \sin(\omega'_{d2}t)e^{-t/\tau''_{d2}} \right\} H_e(t). \tag{11}$$

In accordance with Eq. (11) the important role in AO detection is played by the complex function $D = \frac{C(\partial k_{d2}/\partial\eta)}{(k_{d2} - k''_{g2})}$. The acoustic transients controlled by the AO detection only, i.e., independent of the duration $\tau''_{g2}$ of the photogenerated pulses, can be monitored if $|\mathrm{Im}\ D| \geqslant |\mathrm{Re}\ D|$. However, the theoretical result in Eq. (11) also predicts, that in the case $\tau''_{g2} \geqslant \tau''_{d2}$ the short acoustic transients with the duration $\tau''_{d2}$ could be possibly distinguished at the time scale $t \ll \tau''_{g2}$ on the steplike background provided by $e^{-t/\tau''_{g2}} H_e(t) \simeq H_e(t)$ even if $|\mathrm{Im}\ D| \leq |\mathrm{Re}\ D|$. The ratio $|\mathrm{Im}\ D|/|\mathrm{Re}\ D|$ controlling the profile of the AO detected reflectivity signal strongly depends on the wavelength of the probe optical radiation. Optical properties of the film and the substrate, acousto-optical parameters of the substrate and interference of the probe light in the transparent film, all depend on the probe light wavelength. Interference phenomena in the film have strong dependence also on the film thickness. In our experiments presented below, to study an opportunity of monitoring coherent high-frequency acoustic phonons through the detection of the ultrashort pulsed transient reflectivity signals in the case where photogenerated acoustic pulses are long, we have been modifying both the probe light wavelength and the film thickness.

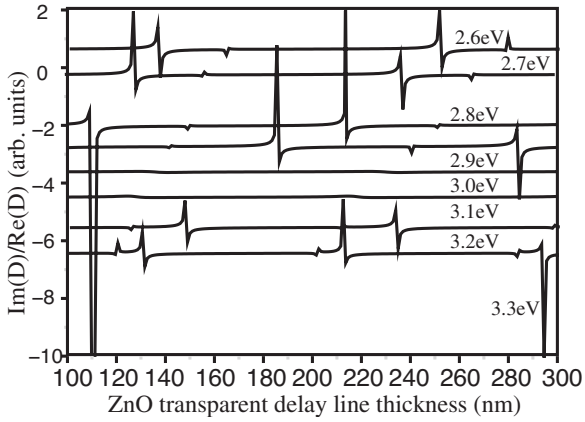


FIG. 3. Calculated ratio Im$(D)$/Re$(D)$ versus probe energy and transparent delay line thickness. The curves are shifted according to the vertical axis for clarity. High values of this ratio correspond to favorable physical situations to reveal short optical transient (i.e., high-frequency coherent acoustic phonons). Each curve exhibits resonances coming from the existence of poles in the coefficient C given in Eq. (2). The magnitudes of theses resonances are given in arbitrary units and are controlled by numerical discretization. The refractive index of *GaAs* and its photoelastic coefficients are tabulated (Refs. 31 and 33). The refractive index of *ZnO* is determined along the literature (Refs. 34 and 35)

## III. DESIGN OF SAMPLES AND EXPERIMENTAL SETUP

As underlined in the introduction and in the theoretical part, to succeed in monitoring coherent hypersound there are some favorable conditions due to optical parameters $(k_{d2})$ and to photoelastic coefficients $(\partial k_{d2}/\partial\eta)$, which must be fulfilled to reveal transients, in time-resolved optical reflectivity, much shorter than the long acoustic strain pulse photoinduced by the pump beam. Using the tabulated values of GaAs photoelastic coefficients versus probe wavelength,[31,32] we have first performed numerical calculations of the ratio Im$(D)$/Re$(D)$ versus probe energy and transparent delay line thickness (Fig. 3). These simulations show that the ratio Im$(D)$/Re$(D)$ is extremely sensitive to these two parameters and can vary by few orders of magnitude. In particular, we show that there are some resonant situations where the ratio Im$(D)$/Re$(D)$ is greatly enhanced.

Nevertheless, as pointed out in the theoretical part, even out of a resonant condition, it still remains possible that the transient reflectivity reveals short optical reflectivity transients providing $\tau''_{d2}$ is enough small compared to $T_{B2}$. Therefore, taking the tabulated optical properties of GaAs[33] and longitudinal sound speed within GaAs $(v_{a2} = 4800\ ms^{-1})$, we have estimated these characteristic times associated to the detection process described in Eq. (11). The results are shown in Fig. 4(a). Interestingly, these results show that in the UV range, the characteristic time $\tau''_{d2}$ becomes smaller than $T_{B2} = 2\pi/\omega'_{d2}$, indicating that in that optical range, broadband detection can be achieved and high frequency coherent acoustic phonons can be monitored. A complete calculation shows indeed in Fig. 5(a) that for a ZnO transparent delay line of 180 nm (corresponding to one of the experimental situation discussed later), short pulsed reflectivity

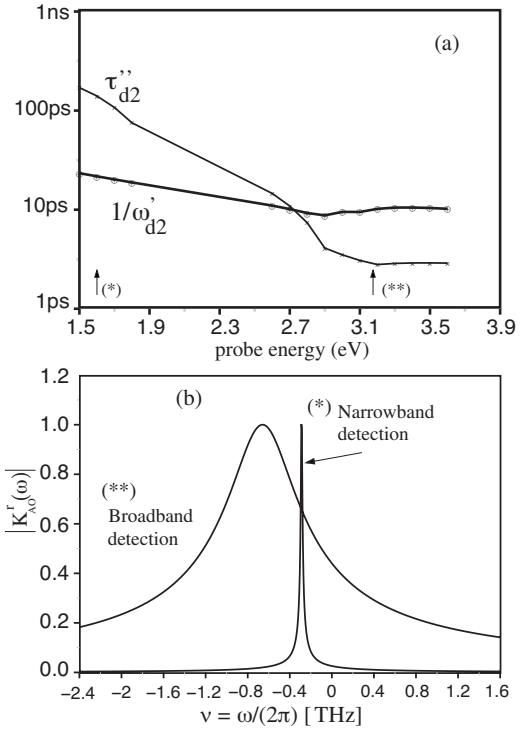


FIG. 4. (a) Characteristic times of detection process versus probe energy in GaAs. $T_{B2}=2\pi/\omega'_{d2}$ is the characteristic period of the Brillouin pulsation at frequency $\omega'_{d2}$. $\tau''_{d2}=(2k''_{d2}v_{a2})^{-1}$ is the characteristic time associated to the ultrasound propagation time across the penetration depth of probe light and it strongly depends on the probe energy quantum. The imaginary part of the optical wave number $k''_{d2}$ is tabulated (Ref. 33) Note that $\tau''_{d2}$ is shorter than $T_{B2}$ in the UV range. (b) spectrum of the AO transfer function for two different probes energies labeled by ( *) and ( **).

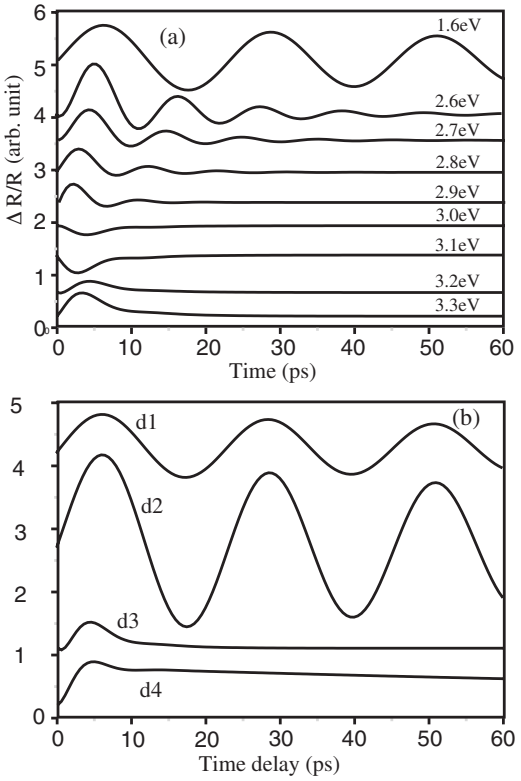


FIG. 5. (a) Time and probe quantum energy dependence of the theoretical photoelastic contribution to the transient reflectivity [Eq. (11)] of GaAs observed when $\tau''_{g2}=(2k''_{g2}v_{a2})^{-1}=160$ ps (Ref. 33). The longitudinal sound speed within GaAs is $v_{a2}=4800\ ms^{-1}$ and the transparent ZnO delay line thickness is 180 nm. These calculations show a transition from a narrowband (probe energy at 1.6 eV) to a broadband detection process (probe energy at ~3.0–3.3 eV). (b) Theoretical transient reflectivity Eq. (11) for different pump-probe configurations. The characteristic times $\tau''_{g2}$, $T_{B2}$ and $\tau''_{d2}$ are: d1(160 ps-22.3 ps-160 ps), d2(6 ps-22.3 ps-160 ps), d3(6 ps-9.5 ps-3 ps), and d4(160 ps-9.5 ps-3 ps). It is confirmed that only small values of $\tau''_{d2}$ enable broadband detection whatever the values of $\tau''_{g2}$ are. The curves are shifted along the vertical axis for clarity.

transients are clearly predicted in the UV range. These theoretical estimates clearly show indeed a transition from a narrowband (Brillouin frequency at $1/T_{B2}\sim 44$ GHz) to a relatively broadband spectrum detection process ($1/\tau''_{d2}\sim 330$ GHz) when we tune the probe wavelength from visible range (1.6 eV) to the UV range. In particular, in the range 3.0–3.3 eV, a short transient in the detected signal is well observed. In these transient reflectivity theoretical calculations we have considered a deeply penetrating pump beam with $\tau''_{g2}$ much greater than the other characteristic times $\tau''_{d2}$ and $T_{B2}=2\pi/\omega'_{d2}$. We have considered the case of an optical excitation by a fixed pump energy of 1.6 eV with $\tau''_{g2}=(2k''_{g2}v_{a2})^{-1}\approx 160$ ps while $\tau''_{d2}$ and $T_{B2}$ vary accordingly to Fig. 4(a). We finally show in Fig. 5(b) that the detected theoretical transient reflectivity time profile drastically depends on the respective value of $\tau''_{d2}$ and $T_{B2}$ and not on $\tau''_{g2}$.

Based on these simulations and predictions, different samples were then prepared. In our studies, we have chosen to work with two systems, namely, ZnO-GaAs and $SiO_2$-GaAs. The samples were prepared using [100] oriented GaAs wafers with high ($n_0\simeq 10^{18}$ cm$^{-3}$) or low ($n_0\simeq 10^{16}$ cm$^{-3}$) doping level. In the first three samples, a film of ZnO was deposited on GaAs by reactive radio frequency magnetron sputtering. Two different processes of sputtering were used. Process 1 consisted in sputtering of a polycrystalline target of sintered ZnO, while in the process 2 metallic Zn was sputtered in oxygen enriched atmosphere to form ZnO. The highly doped samples numbered 1 and 2 are obtained by the process 1 and 2, respectively, and differ in thickness H of the ZnO film (180 and 280 nm, respectively). The low-doped sample 3 of $H=280$ nm was prepared by the process 2. The comparison of the quality of the ZnO/GaAs interface and of free GaAs surface using Raman spectroscopy (a depth of around 50 nm was analyzed under the surface of GaAs with the spectrometer wavelength $\lambda=458$ nm) and x-ray reflectivity (Xpert Philips, $K_\alpha$ Cu) for sample 1, demonstrating that sputtering does not introduce additional defects or residual stresses in GaAs. A native thin oxide layer of 3 nm thickness was detected onto GaAs as expected.[37] For the sample number 4, $SiO_2$ layer was deposited by chemical vapor deposition (CVD) onto low-doped GaAs substrate instead of ZnO in order to have a complete set of different experimental systems.

A classical pump-probe optical setup was used to monitor transient reflectivity spectra of photoexcited samples. A

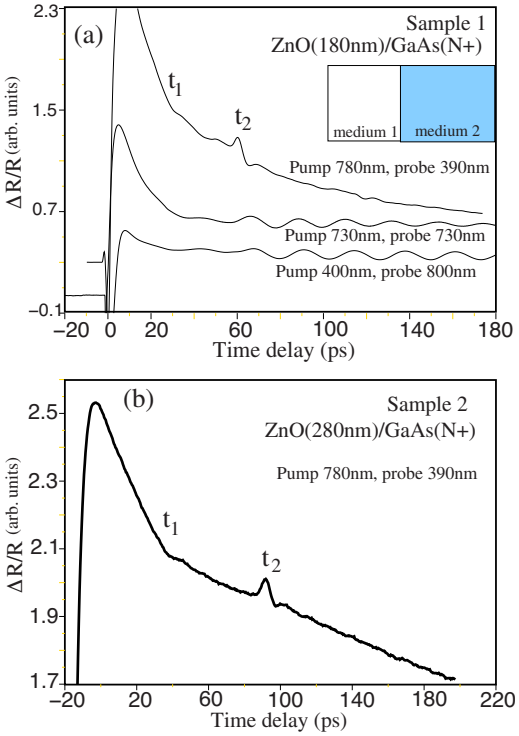


FIG. 6. (Color online) (a) Transient reflectivity signal obtained for sample 1 [ZnO(180 nm)/GaAs]. Two colors pump-probe experiments (top to bottom): pump(3.18 eV)-probe(1.59 eV), 1.59–1.59 eV, 3.1–1.55 eV. (b) Transient reflectivity signal obtained for sample 2 (pump (1.59 eV/780 nm)-probe (3.18 eV/390 nm). In both Figs. 6(a) and 6(b) a clear short pulsed transient reflectivity is detected after a round trip of the acoustic pulse within the ZnO delay line when UV radiation is used for probing transient reflectivity. In (b) a clear kink appears at a time delay $t_1$ equal to half of the delay time for pulse return at the interface. That kink is the signature of the arrival of the acoustic front at the interface air/ZnO.

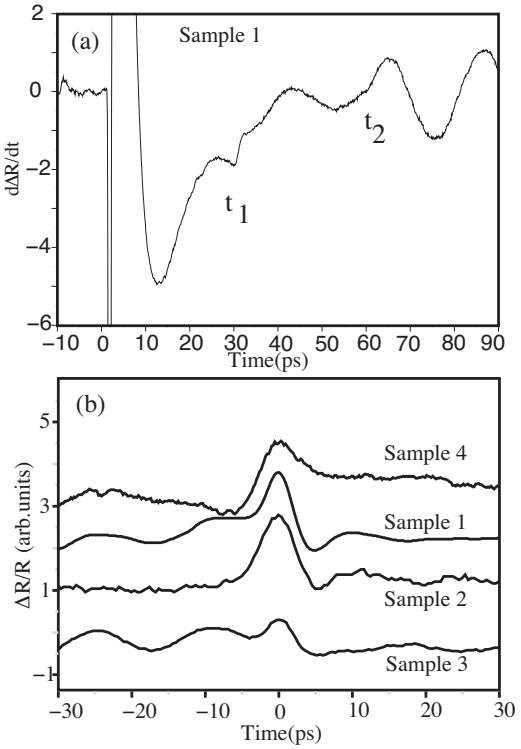


FIG. 7. (a) Time derivative of the signal recorded for sample 1 in the configuration 1.7 eV(730 nm)/1.7 eV(730 nm). At $t=t_1$ (arrival of the acoustic front at the interface air/ZnO), a clear short transient is observed. (b) Presentation of all short acoustic pulses detected in different samples for the configuration pump(1.59 eV/780 nm)-probe(3.18 eV/390 nm).

mode-locked Ti-Sapphire fs laser with pulse repetition rate of 76 MHz and an opportunity to tune the energy of the optical quanta in the red interval 1.41 eV$\leq h\nu_L \leq$1.73 eV was employed. Generation of the second optical harmonic was achieved in a BBO crystal. Note that due to a wide energy gap of ZnO($E_g^{\mathrm{ZnO}} \simeq 3.3$ eV) (Ref. 34) and $SiO_2$($E_g^{\mathrm{SiO_2}} \simeq 9$ eV) the deposited films are transparent for radiation used in our experiments and only GaAs ($E_g^{\mathrm{GaAs}} \simeq 1.43$ eV) can be photoexcited directly.[35] These conditions are required to use ZnO and $SiO_2$ films only as acoustic delay lines and not for sound photogeneration.

## IV. EXPERIMENTAL RESULTS

In order to provide the experimental confirmations of the previous theoretical predictions, we have performed experiments using different combinations of light colors for pump and probe to tune the detection process from the visible to the UV range accordingly to Fig. 4(a). The results are presented in Fig. 6(a) for the sample 1 first [ZnO($H$ =180 nm)/GaAs]. The signals obtained with either a pump in the near UV (3.1 eV/400 nm) or in the visible range (1.7 eV/730 nm) are composed of a slow decaying baseline due to thermal diffusion and photoexcited carriers relaxation. For the two curves in the bottom of Fig. 6(a), clear oscillations of acoustic nature are evidenced and are specially well observed after $t_2 \approx 60$ ps$\approx 2H/v_{a2}$ corresponding to the time where the acoustic pulse, initially generated within the GaAs substrate, comes back to the GaAs substrate after a round trip inside the ZnO transparent layer. Consistently with predictions [Fig. 5(b)], independently of whether the pump optical radiation is deeply ($\tau''_{g2}$=160 ps for a pump wavelength of 730 nm) or weakly ($\tau''_{g2}$=6 ps for a pump wavelength of 400 nm) penetrating, the Brillouin component at ~44 GHz dominates when the detection is done with deeply penetrating probe beam [$\tau''_{d2}$ is 160 ps for a probe beam wavelength (energy) of 730 nm (1.7 eV)]. For these two pump configurations the acoustic part of the transient reflectivity signal corresponds to the well-known ~44 GHz Brillouin frequency.[14,20] The Brillouin scattering in *ZnO* film was not observed due to weak acousto-optic interaction in *ZnO*.[18]

However, it is worth to be noted that a differentiation of the signal obtained for the degenerated configuration 730 nm—730 nm brings into prominence the existence of sharp temporal transient at $t_1 \approx H/v_{a1} \approx 30$ ps [Fig. 7(a)], corresponding to the arrival of the acoustic pulse at the free ZnO surface, indicating that high frequency components are clearly photogenerated and can then be detected. Even if this signal processing provides opportunity to reveal a short optical transient at $t_1 \approx 30$ ps, no clear short optical transient is

detected once the acoustic front comes back to the GaAs substrate at $t=t_2\simeq 60$ ps after a round trip of the acoustic waves inside the ZnO film because of the predominance of the Brillouin signal component.

Experiments achieved by keeping the same deeply penetrating pump light (780 nm) but with a weakly penetrating probe light in the UV range (390 nm), exhibit completely different signals [Fig. 5(a)]. Accordingly to the previous prediction, these new experiments show that short pulsed transient responses of duration $\tau_a^{exp}\simeq 7$ ps corresponding to the arrival of the acoustic waves at $t=t_2$ at the ZnO/GaAs interface are clearly monitored and provide the confirmation that it is possible to detect high frequency components. These short transients are also well confirmed through the experiment achieved with sample 2 [Fig. 6(b)]. We can mention that at $t=t_1$, a change of the slope of the transient reflectivity signal (kink) appears for sample 1 and 2 but particularly better observed for sample 2 [Fig. 6(b)]. A numerical differentiation of the signal shown in Fig. 6(b) also reveals a short transient and confirms the results presented in Fig. 7(a). This singularity, occurring when the acoustic front arrives at the free ZnO surface, is due to a modification of optical interferences between probe beams (in particular the probe beams reflected at the free surface and that at the ZnO/GaAs interface) induced when the acoustic strain turns from a compressive into an tensile field after the reflection on the free ZnO surface. This contribution to the transient reflectivity signal will be reproduced in details later by numerical simulation.

The observation of pulse-shaped transient optical reflectivity for the configuration pump (780 nm)-probe (390 nm) is also well confirmed with the experiments done with samples 3 (ZnO/GaAs) and 4($SiO_2$/GaAs) performed in the same experimental conditions as those employed for samples 1 and 2. After subtracting the baseline and by centering the maximum of the amplitude of each of these short acoustic signals to zero time, we have presented all the results in the Fig. 7(b). Depending on the quality of the polycrystalline ZnO film, it appears that the Brillouin oscillations in ZnO film are observed (sample 1 and 3) or not (sample 2).

## V. ANALYSIS AND DISCUSSION

We have observed in the above presented results that the acoustic components detected are very sensitive to the probe wavelength and less to the pump wavelength as predicted [Figs. 5(a) and 5(b)]. By changing only the probe wavelength we have been able to detect different components of the photogenerated acoustic spectrum from ~44 GHz up to ~100–300 GHz for a fixed OA spectral transformation (same pump wavelength). On the opposite, by changing only the pump wavelength (same AO spectral transformation) from the visible range (730 nm) to the UV range (390 nm) we have not been able to detect indeed different components of the photogenerated acoustic spectrum and mainly single frequency Brillouin oscillations have been clearly resolved (~44 GHz). The observation of the Brillouin oscillations at ~44 GHz for a visible probe light is well known but the observation of short picosecond pulsed transient reflectivity responses produced by deeply penetrating pump radiation and detected with weakly penetrating probe radiation is the major result of our experiments. Such a short transient reflectivity signal related to high-frequency coherent acoustic phonons has never been reported for GaAs before. We show in the following part, through complete numerical simulations taking into account both the OA and the AO processes, that the theoretical prediction proposed in part I [see Eq. (11)] is perfectly relevant to account for the experimental observations.

### A. Laser generated acoustic phonon spectrum

To confirm the theoretical predictions and explanations, and to reproduce numerically the entire experimental signals, it is first necessary to describe the spectral transformation of light intensity envelope in the OA conversion (i.e., the photogenerated phonons spectrum) achieved with deeply penetrating pump beam (780 nm) and to show that the theoretical assumption of Eq. (8) is relevant for our experimental conditions. We first recall that the generation of the acoustic waves in GaAs is dominated by the stresses induced by the photogenerated e-h plasma through electron-hole-phonon deformation potential.[7,14,20,38]

The acoustic phonon spectrum has been calculated following previous theoretical modeling.[8] The expression of $\eta(\omega)$ is given by:[7,8,38]

$$\eta(\omega)=\frac{-i\omega}{v_{a2}(1+N_{12})}\times\frac{(1-R)I\tilde{f}(\omega)}{h\nu_L\rho v_{a2}^2}\times\frac{-d_{\mathrm{eh}}}{\rho_2 v_{a2}^2}\times\frac{m_{D_{\mathrm{eh}}}\omega_{D_{\mathrm{eh}}}}{(m_{D_{\mathrm{eh}}}\sqrt{\omega_{D_{\mathrm{eh}}}}+\sqrt{-i\omega})\sqrt{-i\omega}(\sqrt{\omega_{D_{\mathrm{eh}}}}+\sqrt{-i\omega})}+\left[\frac{1}{\sqrt{-i\omega}}+\frac{\sqrt{\omega_{D_{\mathrm{eh}}}}}{\omega_{\alpha_{g2}}-i\omega}\right],\tag{12}$$

where $\omega_{D_{\mathrm{eh}}}=\frac{v_{a2}^2}{D_{\mathrm{eh}}}$, $m_D=\frac{\alpha_{g2}D_{\mathrm{eh}}}{v_{a2}}$, $\omega_R=\frac{1}{\tau_R}$ (we recall that the number 1 and 2 refer to ZnO film and GaAs substrate, respectively). $v_{a2}$, $D_{\mathrm{eh}}$, $\tau_R$, $\rho_2$, $R$, and $d_{\mathrm{e\text{-}h}}$ are, the longitudinal sound speed in GaAs, the carriers ambipolar diffusion coefficient, the characteristic time of bulk recombination, the density, the optical reflectivity coefficient and the deformation potential parameter, respectively. For the calculation, we have chosen the usual values of $D_{\mathrm{eh}}=3.3$ $\mathrm{cm^2s^{-1}}$, $\tau_R\approx 1$ ns, and $d_{\mathrm{e\text{-}h}}=10$ eV (Refs. 14, 20, and 38) and for the optical absorption coefficient the tabulated data.[33] $N_{12}$ is the ratio of the acoustic impedances *ZnO/GaAs* defined as $N_{12}=\rho_1 v_{a1}/\rho_2 v_{a2}$ where $v_{a1}$ and $\rho_1$ are the longitudinal sound speed in ZnO and the density of ZnO and $\rho_2$ is the density of GaAs. $I$ and $\tilde{f}(\omega)$ are the pump pulse intensity and the spectrum of femtosecond pump pulse intensity envelope. The calculated spectra are given for both near-IR (780 nm) and, for the comparison, for near-UV (400 nm) pump radiation in Fig. 8. As expected, the near-UV radiation provides more high-frequency components even if electronic ambipolar diffusion diminishes these components due to a spatial broadening of electron-hole plasma localization region.[14] For red pump light, both the effect of carrier bulk recombination and

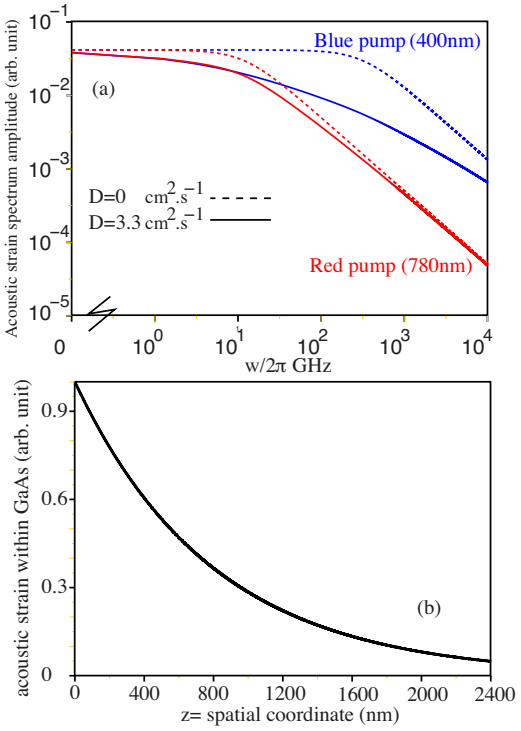


FIG. 8. (Color online) (a) amplitude of the spectrum of the photogenerated acoustic pulse for a pump wavelength of 780 nm and 390 nm. The details of the calculation of this spectrum are given in the text. (b) Exponential spatial profile of acoustic strain pulse launched in ZnO after being generated within GaAs with a pump wavelength (energy) of 780 nm (1.59 eV). This pure exponential decay corresponds, in the frequency domain, to the approximate amplitude of acoustic strain spectrum given in Eq. (9) ($|\tilde{\eta}(\omega)| \approx [\omega^2 + \omega_{g2}''^2]^{-1/2}$)

the carrier ambipolar diffusion are negligible in the GHz–THz frequency range of interest here. Consequently, the photogenerated pulse exhibits a simple exponential decay [Fig. 8(b)]. This justifies the relevance of Eqs. (8) and (9) employed for the theoretical prediction made for GaAs. When analyzing the spectrum [Fig. 8(a)], it appears that the theory predicts a broad spectrum for the photoexcited sound. It means that the frequency 44 GHz corresponding to so-called Brillouin oscillations and even those contained in the detected transient reflectivity (i.e., ~100–300 GHz) both exist. In particular, at $\omega > \omega_{d2}''$, $|\tilde{\eta}(\omega)| \sim 1/\omega$ and, consequently, the acoustic spectral components at frequency of $f \sim 200$ GHz $\sim 5 f_B$ are only five times weaker than the component at Brillouin frequency ($f_B \sim 44$ GHz). This clearly shows that the OA spectral transformation is not the limiting process and this confirms again that the detection process (AO process) clearly determines which component will be observed during experiments.

Taking into account the law of acoustic reflection and transmission at the interface ZnO-GaAs (no attenuation was taken into account) it is then possible to simulate the time dependence of the acoustic strain bouncing back and forth in the ZnO layer. For longitudinal wave propagating in the [100] direction for GaAs and along $C_6$ axis for ZnO we have $Z_{GaAs} = 2.55.10^7$ kgm$^{-2}$s$^{-1}$ and $Z_{ZnO} = 3.42.10^7$ kgm$^{-2}$s$^{-1}$ respectively. It is to be noted that after a round trip, nearly all the mechanical energy is transferred into GaAs substrate since the impedance of the two materials are close.

### B. Simulation of the entire time-dependent transient reflectivity signal in the ZnO/GaAs system

Once the spatial and time dependence of the acoustic strain is simulated, it is then possible to calculate the theoretical transient reflectivity following Eq. (1).[8] Since experimentally we measure a variation of the modulus of the optical reflection coefficient $R = rr^*$, we have then calculated the real part of $\Delta r(t)/r_0 = \Delta A/A + i\Delta\phi$ as $\Delta R/2R = \mathrm{Re}(\Delta r(t)/r_0) = \Delta A/A$. The simulations were performed for the so-called red-blue configurations where the pump and probe wavelength were 390–780 nm (3.18 eV–1.59 eV) and 400–800 nm (3.1 eV–1.55 eV). For these couples of wavelengths, the optical refractive index is 2.05 (390 nm and 400 nn) for ZnO and $3.93 + 2.28i$ (390 nm) and $4.3 + 2.14i$ (400 nm) for *GaAs*.[33] Some photoelastic coefficients are tabulated for low doped GaAs($10^{16}$ cm$^{-3}$).[31] For ZnO, a lot of studies have been performed to measure the photoelastic coefficients. In spite of these numerous studies, it is very difficult to find some confirmed values of the photoelastic coefficients and especially in the UV range. The photoelastic coefficients are very sensitive to the quality of crystals. While for GaAs the optimization of single crystal growth is well controlled, for polycrystalline ZnO material it is not. Consequently, different values and significant discrepancies appear in the literature. To our best knowledge, the only data measured close to the wavelength chosen in our experiment are those measured by Carlotti *et al.*[39] at 488 nm. Additional data can also be found from Tell *et al.*[40] and Vedam *et al.*[41] We have finally found that $\frac{dn}{d\eta}$ ranges between ~1 and ~8. For our simulation and since *ZnO* transparent film were not annealed to protect the GaAs substrate from oxidation damages, we have chosen the lowest value i.e., $\frac{dn}{\eta}_{\mathrm{ZnO}=1}$.

In Fig. 9(a), the simulated transient reflectivity signal $\Delta R/2R$ is shown for two pump-probe configurations. In these signals we can identify different contributions [the slow decay clearly observable on the experimental transient reflectivity (Fig. 6) is of thermal and electronic origin and is not simulated here]. First of all, for $0 < t < 60$ ps, there are the oscillations assigned to Brillouin scattering within the GaAs substrate and within ZnO layer (weaker contribution from ZnO). Second, the dashed line shown in this figure comes from the contribution of the first integral in Eq. (1). It is a contribution of a well-known interferometric nature.[8,23] The pump pulse penetration depth (~750 nm at a pump wavelength of 780 nm) is larger than the ZnO layer thickness (180 nm), consequently, through the transient reflectivity, it is possible to monitor in the time domain the optical effect of a continuous compression ($0 < t < t_1$) and an expansion ($t_1 < t < t_2$) of the ZnO layer submitted to a long acoustic strain pulse which bounces back and forth within the transparent ZnO layer. Submitted to an acoustic field the ZnO layer thickness H decreases first and after the acoustic reflection on the free surface (inversion of the sign of the acoustic strain) that layer thickness increases. That geometrical effect

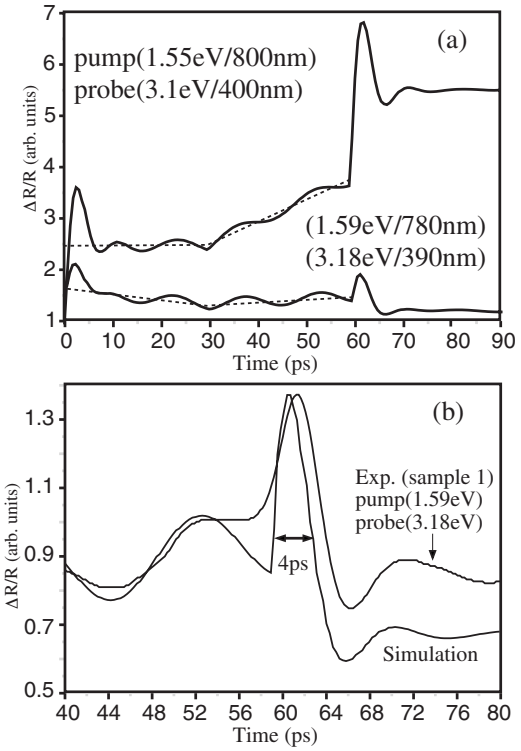


FIG. 9. (a) Simulation of the transient reflectivity signal $\Delta R/R$ in the configuration pump (1.55 eV-800 nm)/probe (3.1 eV-400 nm) (top curve) and pump (1.59 eV-780 nm)/probe (3.18 eV-390 nm) (bottom curve). For these simulation the optical parameters as well as the photoelastic coefficients used for ZnO are $n_{\mathrm{ZnO}}=2.05$ and $\frac{dn}{d\eta})_{\mathrm{ZnO}}=1$ whatever the probe wavelength. For GaAs we used for the probe wavelength of 390 nm and 400 nm, $n_{\mathrm{GaAs}}=3.93+2.28i$ and $n_{\mathrm{GaAS}}=4.3+2.14i$, and $\frac{dn}{d\eta})_{\mathrm{GaAs}}=19.7+5.6i$ and $\frac{dn}{d\eta})_{\mathrm{GaAs}}=39+44.5i$.(b) A comparison between experiment (sample 1) and the simulated transient reflectivity obtained with the same optical and photoelastic parameters used in (a) for the probe wavelength of 390 nm: the agreement is reasonable for these set of parameters.

has a direct consequence on the reflected optical signal and acts as a Fabry-Perot resonator effect. In Fig. 6(b), it is well characterized as a function of time by the kink observed at $t=t_1$. Note that in the case of acoustic strain with spatial extension smaller than the film thickness, a jump is observed on the signal rather than a kink.[23] We can show that the derivative of this interferometric signal provides a step like signal which explains the short transient observed at $t=t_1$ in Fig. 7(a). Furthermore, these complete simulations clearly reproduce some fast components distinguished by two pulsed transients at $t\sim 4$ ps and at $t\sim 60$ ps. They correspond to the photoelastic coupling between the propagating acoustic pulse and probe light within GaAs substrate. These photoelastic contributions within the GaAs substrate correspond to the third term in Eq. (1). We have found that for a given couple of values of photoelastic coefficients for ZnO and GaAs compounds it is possible to reproduce with a good agreement the transient reflectivity signal. Especially for sample 1 and with $\frac{dn}{d\eta})_{\mathrm{GaAs}}=19.7+5.6i$ (probe at 390 nm) and $\frac{dn}{d\eta})_{\mathrm{ZnO}}=1$ the simulation of the shape of the detected acoustic echo is pretty good [Fig. 9(b)]. Nevertheless, we were not able to reproduce the entire shape of the detected transient acoustic signal by taking directly the tabulated photoelastic coefficients which were obtained for undoped GaAs sample.[31] It is to be mentioned indeed that the simulations (Fig. 9) reveal, in accordance with the literature,[16,42] that a slight change of the probe wavelength (and hence of the photoelastic coefficients) importantly modifies the magnitude of the pulse shaped optical transient detected at $t=t_2$. Similarly, for a given probe wavelength, if there is a slight variation of the electronic structure from one sample to another sample, then it might lead also to a variation of the detected signal. In our measurements, we have observed that the largest magnitude of short pulsed transient reflectivity signal related to high frequency coherent acoustic phonons was obtained with doped GaAs (sample 1 and 2) while for the low-doped sample (number 3), that magnitude was smaller. Therefore, we think that the variations observed experimentally come from a difference between photoelastic coefficients, which are not equivalent in all samples due partially to different doping levels at least. That point is consistent with recent results obtained in the visible range in differently doped GaAs samples.[43]

### C. Key role of the sharp leading acoustic front

The simulations of the time-dependence of the transient reflectivity in the system ZnO-GaAs, taking into account a classical deeply penetrating exponential-shaped photogenerated stress, demonstrate that we can account for the observed short pulsed transient optical reflectivity signal.

It is worth to recall that according to the spectrum established before (Fig. 8) the main components of photogenerated sound are situated below 10 GHz but the spectrum contains also high frequencies. We show in the next simulations that these high frequency components, that we are able to detect and to simulate, are contained in the sharp leading front of the propagating acoustic pulse and, if we suppress them from the OA spectrum, we consequently make the short optical transient disappear. We have simulated the transient reflectivity signal for different acoustic strain profiles incident to GaAs substrate [shown in Fig. 10(a)], starting from an ideal sharp leading front (number 1) toward attenuated acoustic leading front (2, 3, and 4). The leading acoustic front time-profile was tailored according to the expression $\eta(t-z/v_{a2})=\eta_0\{-\exp[-(t-z/v_{a2})/\tau''_{g2}]+\exp[-(t-z/v_{a2})/\tau_a]\}$ where $\tau''_{g2}\approx 160$ ps (characteristic time associated to a photoexcitation by a deeply penetrating pump at 780 nm) and $\tau_a$ is a characteristic time associated to the phonon cut-off frequency $\omega_a\approx 1/\tau_a$ ($|\tilde{\eta}(\omega)|\sim(\omega^2+\omega''^2_{g2})^{-1/2}(\omega^2+\omega_a^2)^{-1/2}$). For the profile (1) to (4), $\tau_a$ is 0, 5.3, 8, and 16 ps, respectively. The calculated transient reflectivity is shown in Fig. 10(b). It appears clearly that only a very sharp front can reasonably reproduce the transient reflectivity pulse we have detected. These simulations clearly confirm the original experimental observation that even with deeply penetrating pump beam, high frequency components ($>200$ GHz) can be not only generated by deeply penetrating pump light but can also be detected thanks to a weakly penetrating probe light.

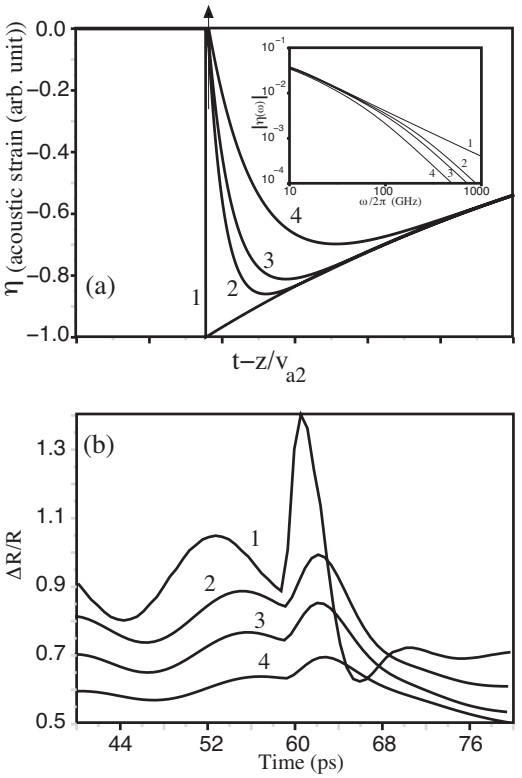


FIG. 10. (a) Different photoinduced acoustic strain time-profile incident on *GaAs* substrate: sharp to smooth leading acoustic front (the corresponding acoustic spectrum amplitude (arb. unit) is given in the inset). For this simulated optical transient we took: $n_{\mathrm{ZnO}}=2.05$, $\frac{dn}{d\eta})_{\mathrm{ZnO}}=1$, $n_{\mathrm{GaAs}}=3.93+2.28i$, and $\frac{dn}{d\eta})_{\mathrm{GaAs}}=19.7+5.6i$ (b) transient reflectivity signal simulated with the four previous acoustic strain profiles. The reduction of high-frequency component through the leading acoustic front broadening clearly makes the short acoustic pulse vanish. The analytical expression of leading acoustic fronts (1) to (4) time-profiles expressions in (a) are given in the text.

## VI. CONCLUSIONS

As a summary, we have revisited the theory of detection process for ultra-fast acoustics using frequency domain analysis. For that, we specially focused on the description of detection spectral transformation function [i.e., AO spectral transformation function]. We have shown that it is possible to monitor high frequency coherent acoustic phonons through the detection of ultrashort transient reflectivity pulsed signals, even if the photoinduced acoustic strain has a characteristic duration much longer than picosecond time scale. For example, we experimentally evidenced that it is possible to tune the acousto-optic spectral transformation function from a narrowband to a broadband detection process in GaAs. With a long strain pulse (characteristic pulse duration of ~160 ps) we have then succeeded indeed in monitoring either the Brillouin mode at ~44 GHz (characteristic time of ~22 ps) with a deeply penetrating probe centered on 730 nm or 800 nm or in probing high frequency phonons of typical frequency ranging between ~100 and ~300 GHz (characteristic time included between 3 and 10 ps) with a weakly penetrating probe (penetration depth ~15 nm). We have established and explained that the broadband detection process is achieved as soon as the characteristic time of phonon propagation over the optical penetration depth of probe light $\tau_d''$ is shorter that the characteristic time of phonon propagation over the optical wavelength of the probe beam $T_B=2\pi/\omega_B$ (where $\omega_B$ is the Brillouin frequency). The transient reflectivity pulsed signal we have detected is of the same order of duration as that detected in metals,[1,18,21,44,45] in heterostructures containing $GaAs/Al_{0.3}Ga_{0.7}As$ nanometric quantum wells,[46] or of the same order as solitons.[47–49] This study clearly confirms that it is really important in laser ultrasonics to have a proper detection configuration (proper wavelength, high photoelastic coefficients) to reveal high frequency coherent acoustic phonons.

## ACKNOWLEDGMENTS

This work was supported by ANR–BLAN06–3–136286 GHzOCPETS. The authors are grateful to A. Bulou for valuable discussions and Raman spectroscopy analysis.

## APPENDIX

List of the notations frequently used in the text:

$v_a$ is the acoustic phonon velocity.

$k_g$, $k_g'$, and $k_g''$ are the wave numbers of the pump optical radiation generating the acoustic waves, its real and imaginary parts.

$\omega_g=\omega_g''=2k_g''v_a$ is the characteristic cyclic frequency of the photogenerated acoustic waves.

$\tau_g=\omega_g^{-1}$ is the characteristic duration of the photogenerated acoustic pulse, which is equal to the time of acoustic wave propagation across the pump intensity penetration depth.

$k_d$, $k_d'$ and $k_d''$ are the wave numbers of the probe optical radiation detecting the acoustic waves, its real and imaginary parts.

$\omega_d=-2ik_dv_a=\omega_d'+\omega_d''$ is the characteristic cyclic frequency of the detected acoustic waves contributing to the transient reflectivity signal.

$\omega_d'=\omega_B=$is the cyclic Brillouin frequency. $T_B=2\pi/\omega_B$ is the corresponding Brillouin period.

$\tau_d'=(\omega_d')^{-1}$ is the characteristic time proportional to the duration of the acoustic wave propagation across the depth equal to the probe light wavelength.

$\tau_d''=(\omega_d'')^{-1}=(2k_d''v_a)^{-1}$ is the characteristic time equal to the duration of the acoustic wave propagation across the detection region determined by the probe laser radiation penetration.

*pascal.ruello@univ-lemans.fr


[1] C. Thomsen, H. T. Grahn, H. J. Maris, and J. Tauc, Phys. Rev. B **34**, 4129 (1986).

[2] H. T. Grahn, H. J. Maris, and J. Tauc, IEEE J. Quantum Electron. **25**, 2562 (1989).

[3] H. N. Lin, R. J. Stoner, H. J. Maris, and J. Tauc, J. Appl. Phys. **69**, 3816 (1991).

[4] S. A. Akhmanov and V. E. Gusev, Sov. Phys. Usp. **35**, 153 (1992).

[5] C. Thomsen, J. Strait, Z. Vardeny, H. J. Maris, J. Tauc, and J. J. Hauser, Phys. Rev. Lett. **53**, 989 (1984).

[6] C. Thomsen, H. T. Grahn, H. J. Maris, and J. Tauc, Opt. Commun. **60**, 55 (1986).

[7] V. Gusev and A. Karabutov, *Laser Optoacoustics* (AIP, New York, 1993).

[8] V. Gusev, Acustica Acta Acust. **82**, S37 (1996).

[9] G. Tas and H. J. Maris, Phys. Rev. B **49**, 15046 (1994).

[10] V. Gusev, Opt. Commun. **94**, 76 (1992).

[11] O. B. Wright and V. Gusev, IEEE Trans. Ultrason. Ferroelectr. Freq. Control **UFFC-42**, 331 (1995).

[12] V. E. Gusev and O. B. Wright, Phys. Rev. B **57**, 2878 (1998).

[13] N. V. Chigarev, D. Yu. Paraschuk, X. Y. Pan, and V. E. Gusev, Phys. Rev. B **61**, 15837 (2000).

[14] O. B. Wright, B. Perrin, O. Matsuda, and V. E. Gusev, Phys. Rev. B **64**, 081202(R) (2001).

[15] A. Devos and R. Cote, Phys. Rev. B **70**, 125208 (2004).

[16] A. Devos and A. Le Louarn, Phys. Rev. B **68**, 045405 (2003).

[17] C. Rossignol, J. M. Rampnoux, T. Dehoux, and B. Audoin, Rev. Sci. Instrum. **77**, 033101 (2006).

[18] T. Pezeril, P. Ruello, S. Gougeon, N. Chigarev, D. Mounier, J.-M. Breteau, P. Picart, and V. Gusev, Phys. Rev. B **75**, 174307 (2007).

[19] O. B. Wright, B. Perrin, O. Matsuda, and V. E. Gusev, Phys. Rev. B **78**, 024303 (2008).

[20] O. Matsuda, O. B. Wright, D. H. Hurley, V. Gusev, and K. Shimizu, Phys. Rev. B **77**, 224110 (2008).

[21] T. Pezeril, N. Chigarev, P. Ruello, S. Gougeon, D. Mounier, J.-M. Breteau, P. Picart, and V. Gusev, Phys. Rev. B **73**, 132301 (2006).

[22] O. B. Wright and T. Hyoguchi, Opt. Lett. **16**, 1529 (1991).

[23] O. B. Wright, J. Appl. Phys. **71**, 1617 (1992).

[24] C. Rossignol, B. Perrin, S. Laborde, L. Vandenbulcke, M. I. De Barros, and P. Djemia, J. Appl. Phys. **95**, 4157 (2004).

[25] A. Devos, J.-F. Robillard, R. Cote, and P. Emery, Phys. Rev. B **74**, 064114 (2006).

[26] C. Mechri, P. Ruello, J. M. Breteau, M. R. Baklanov, P. Verdonck, and V. Gusev, Appl. Phys. Lett. **95**, 091907 (2009).

[27] R. Côte and A. Devos, Rev. Sci. Instrum. **76**, 053906 (2005).

[28] B. Perrin, C. Rossignol, B. Bonello, and J.-C. Jeannet, Physica B **263-264**, 571 (1999).

[29] O. Matsuda and O. B. Wright, J. Opt. Soc. Am. B **19**, 3028 (2002).

[30] Surely, as soon as the complex frequency spectrum of the acoustic strain field $\tilde{\eta}(\omega)$ contains itself some poles or some brunch lines in the complex $\omega$-plane, the contributions to the Eq. (7) to the time-domain signal, from the considered pole at $\omega=-i\omega_{d2}$ in Eq. (6) is not the only one.

[31] P. Etchegoin, J. Kircher, M. Cardona, C. Grein, and E. Bustarret, Phys. Rev. B **46**, 15139 (1992).

[32] The photoelastic coefficients are found in the work of Etchegoin *et al.* (Ref. 31). These photoelastic coefficients are given in the unity of $Pa^{-1}$. From these $P_{ij}$ coefficients and from the stiffness parameters of *GaAs*, we deduce the photoelastic coefficient as $dn/d\eta=\frac{P_{11}C_{12}+P_{12}C_{11}+P_{12}C_{12}}{2n}$ (Ref. 36) and $dk_{d2}/d\eta=\frac{2\pi}{\lambda_2}dn/d\eta$, where $\lambda_2$ is the probe wavelength. It is to be mentionned that close to 390 nm there is an efficient optical interband transition (Ref. 33). As a consequence, the imaginary part of the refractive index is large and similar to the real part. Moreover, due to a huge energy dependence of the optical refractive index, the photoelastic coefficients exhibit large values in the vicinity of this interband transition.

[33] D. E. Aspnes and A. A. Studna, Phys. Rev. B **27**, 985 (1983).

[34] F. K. Shan and Y. S. Yu, J. Eur. Ceram. Soc. **24**, 1869 (2004).

[35] The refractive index of ZnO from Ref. 34 is given for a probe ranging from 0.7 to 3.0 eV. The refractive indexes for an energy of 3.1–3.3 eV were extrapolated according to the Sellmeier dispersion law.

[36] A. Feldman and R. M. Waxler, J. Appl. Phys. **53**, 1477 (1982).

[37] S. Lodha, D. B. Janes, and N.-P. Chen, Appl. Phys. Lett. **80**, 4452 (2002).

[38] P. Babilotte, E. Morozov, P. Ruello, D. Mounier, M. Edely, J.-M. Breteau, A. Bulou, and V. E. Gusev, J. Phys.: Conf. Ser. **92**, 012019 (2007).

[39] G. Carlotti, G. Socino, and E. Verona, Proc.-IEEE Ultrason. Symp. **1**, 427 (1988).

[40] B. Tell, J. M. Worlock, and R. J. Martin, Appl. Phys. Lett. **6**, 123 (1965).

[41] K. Vedam and T. A. Davis, Phys. Rev. **181**, 1196 (1969).

[42] A. Devos and C. Lerouge, Phys. Rev. Lett. **86**, 2669 (2001).

[43] F. Hudert, A. Bartels, T. Dekorsy, and K. Köhler, J. Appl. Phys. **104**, 123509 (2008).

[44] G. L. Eesley, B. M. Clemens, and C. A. Paddock, Appl. Phys. Lett. **50**, 717 (1987).

[45] T. Saito, O. Matsuda, and O. B. Wright, Phys. Rev. B **67**, 205421 (2003).

[46] O. Matsuda, T. Tachizaki, T. Fukui, J. J. Baumberg, and O. B. Wright, Phys. Rev. B **71**, 115330 (2005).

[47] H.-Y. Hao and H. J. Maris, Phys. Rev. B **64**, 064302 (2001).

[48] E. Peronne and B. Perrin, Ultrasonics **44**, e1203 (2006).

[49] O. L. Muskens and J. I. Dijkhuis, Phys. Rev. Lett. **89**, 285504 (2002).